Contents

1 The Proposed Experiment

1.1 Experimental Method

As in the case for E12-13-011, the measured double differential cross section for a spin-1 target characterized by a vector polarization P_z and tensor polarization P_{zz} is expressed as,

$$\frac{d^2\sigma_p}{d\Omega dE'} = \frac{d^2\sigma_u}{d\Omega dE'}\left(1 - P_z P_B A_1 + \frac{1}{2}P_{zz}A_{zz}\right), \tag{1}$$

where, σ_p (σ_u) is the polarized (unpolarized) cross section, P_B is the incident electron beam polarization, and A_1 (A_{zz}) is the vector (tensor) asymmetry of the virtual-photon deuteron cross section. This allows us to write the polarized tensor asymmetry with $0 < P_{zz} \leq 1$ using an unpolarized electron beam as

$$A_{zz} = \frac{2}{P_{zz}}\left(\frac{\sigma_p - \sigma_u}{\sigma_u}\right), \tag{2}$$

where σ_p is the polarized cross section. The tensor polarization is given by

$$P_{zz} = \frac{n_+ - 2n_0 + n_-}{n_+ + n_- + n_0}, \tag{3}$$

where n_m represents the population in the $m_z = +1$, -1, or 0 state.

Eq. 2 reveals that the asymmetry A_{zz} compares two different cross sections measured under different polarization conditions of the target: positively tensor polarized and unpolarized. To obtain the relative cross section measurement in the same configuration, the same target cup and material will be used at alternating polarization states (polarized vs. unpolarized), and the magnetic field providing the quantization axis will be oriented along the beamline at all times. This field will always be held at the same value, regardless of the target material polarization state. This process, identical to that used for the E12-13-011 b_1 measurement, ensures that the acceptance remains consistent within the stability (10^{-4}) of the super conducting magnet.

Since many of the factors involved in the cross sections cancel in the ratio, Eq. 2 can be expressed in terms of the charge normalized, efficiency corrected numbers of tensor polarized (N_p) and unpolarized (N_u) counts,

$$A_{zz} = \frac{2}{fP_{zz}}\left(\frac{N_p - N_u}{N_u}\right). \tag{4}$$

The dilution factor f corrects for the presence of unpolarized nuclei in the target and is defined by

$$f = \frac{N_D\sigma_D}{N_N\sigma_N + N_D\sigma_D + \sum_A N_A\sigma_A}, \tag{5}$$

where N_D is the number of deuterium nuclei in the target and σ_D is the corresponding inclusive double differential scattering cross section, N_N is the nitrogen number of scattered nuclei with

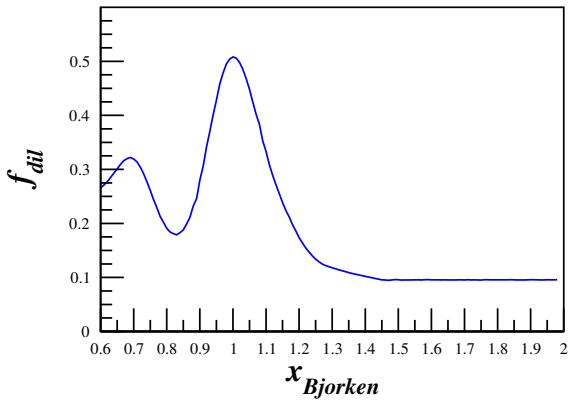

Figure 1: The estimated dilution factor, in this case at $Q^2 = 1.5\ (\mathrm{GeV}/c)^2$, is expected to drop off at high x until it reaches the SRC plateau region. This effect will be counteracted by using a high-luminosity solid target.

cross section σ_N, and N_A is the number of other scattering nuclei of mass number A with cross section σ_A. As has been noted in previous work [1], the dilution factor at high x drops off considerably until the SRC plateau region, as shown in Fig. 1. By using a high-luminosity solid target and a low angle $\theta_{e'}$, this effect will be largely counteracted.

The dilution factor can be written in terms of the relative volume ratio of ND_3 to LHe in the target cell, otherwise known as the packing fraction p_f. In our case of a cylindrical target cell oriented along the magnetic field,the packing fraction is exactly equivalent to the percentage of the cell length filled with ND_3.

If the time is evenly split between scattering off of polarized and unpolarized ND_3, the time necessary to achieve the desired precision δA is:

$$T = \frac{N_p}{R_p} + \frac{N_u}{R_u} = \frac{8}{f^2 P_{zz}^2}\left(\frac{R_p(R_u + R_p)}{R_u^3}\right)\frac{1}{\delta A_{zz}^2} \tag{6}$$

where $R_{p(u)}$ is the polarized (unpolarized) rate and $N_{p(u)}$ is the total estimated number of polarized (unpolarized) counts to achieve the uncertainty δA_{zz}.

1.1.1 Statistical Uncertainty

To investigate the statistical uncertainty we start with the equation for A_{zz} using measured counts for polarized data (N_p) and unpolarized data (N_u),

$$A_{zz} = \frac{2}{f P_{zz}}\left(\frac{N_p}{N_u} - 1\right). \tag{7}$$

The statistical error with respect to counts is then

$$\delta A_{zz} = \frac{2}{f P_{zz}}\sqrt{\left(\frac{\delta N_p}{N_u}\right)^2 + \left(\frac{N_p \delta N_u}{N_u^2}\right)^2}. \tag{8}$$

Source	Systematic
Polarimetry	7.7%
Dilution/packing fraction	4.0%
Radiative corrections	1.5%
Charge Determination	1.0%
Detector resolution and efficiency	1.0%
Total	10%

Table 1: Estimates of the scale dependent contributions to the systematic error of A_{zz}.

For $\delta N_{p(u)} = \sqrt{N_{p(u)}}$, the uncertainty becomes

$$\delta A_{zz} = \frac{2}{f P_{zz}} \sqrt{\frac{N_p(N_u + N_p)}{N_u^3}}, \tag{9}$$

which can't be simplified further due to the large expected asymmetry.

1.1.2 Systematic Uncertainty

Table 1 shows a list of the scale dependent uncertainties contributing to the systematic error in A_{zz}.

With careful minimization, the uncertainty in P_z can be held to better than 4%, as demonstrated in the recent g2p/GEp experiment [2]. This leads to a a relative uncertainty in P_{zz} of 7.7%. Alternatively, the tensor asymmetry can be directly extracted from the NMR lineshape as discussed in Sec. **??**, with similar uncertainty. The uncertainty from the dilution factor and packing fraction of the ammonia target contributes at the 4% level. The systematic effect on A_{zz} due to the QED radiative corrections will be quite small. For our measurement there will be no polarized radiative corrections at the lepton vertex, and the unpolarized corrections are known to better than 1.5%.

Charge calibration and detector efficiencies are expected to be known better to 1%, but the impact of time-dependent drifts in these quantities must be carefully controlled.

Time dependent factors

Eq. 4 involves the ratio of counts, which leads to cancellation of several first order systematic effects. However, the fact that the two data sets will not be taken simultaneously leads to a sensitivity to time dependent variations which will need to be carefully monitored and suppressed. To investigate the systematic differences in the time dependent components of the ntegrated counts, we need to consider the effects from calibration, efficiency, acceptance, and luminosity between the two polarization states.

Fluctuations in luminosity due to target density variation can easily be kept to a minimum by keeping the material beads at the same temperature for both polarization states by control of the microwave and the LHe evaporation. The He vapor pressure reading can give accuracy of material temperature changes at the level of $\sim$0.1%. Beam rastering can also be controlled to a high degree.

The acceptance of each cup can only change as a function of time if the magnetic field changes. The capacity to set, reset, and hold the target superconducting magnet to a desired holding field causes a field uncertainty of only $\delta B/B = 0.01\%$. This implies that, like the cup length l, the acceptance $\mathcal{A}$ for each polarization state is the same.

In order to look at the effect on A_{zz} due to drifts in beam current monitor calibration and detector efficiency, we rewrite Eq. 4 explicitly in terms of the raw measured counts N_p^c and N_u^c,

$$\begin{aligned} A_{zz} &= \frac{2}{fP_{zz}}\left(\frac{N_p^c}{N_u^c} - 1\right) \\ &= \frac{2}{fP_{zz}}\left(\frac{Q\varepsilon l\mathcal{A}}{Q_1\varepsilon_1 l\mathcal{A}}\frac{N_p}{N_u} - 1\right) \end{aligned} \tag{10}$$

where Q represents the accumulated charge, and ε is the detector efficiency. The target length l and acceptance $\mathcal{A}$ are identical in both states to first order.

We can then express Q_1 as the change in beam current measurement calibration that occurs in the time it takes to collect data in one polarization state before switching to another, such that $Q_1 = Q(1 - dQ)$. In this notation dQ is a dimensionless ratio of changes in different polarization states. A similar representation is used for drifts in detector efficiency leading to,

$$A_{zz} = \frac{2}{fP_{zz}}\left(\frac{N_pQ(1-dQ)\varepsilon(1-d\varepsilon)}{N_uQ\varepsilon} - 1\right). \tag{11}$$

which simplifies to,

$$A_{zz} = \frac{2}{fP_{zz}}\left(\frac{N_p}{N_u}(1 - dQ - d\varepsilon + dQd\varepsilon) - 1\right). \tag{12}$$

For estimates of the dQ and $d\varepsilon$ we turn to previous experimental studies. For HRS detector drift during the JLab transversity experiment E06-010, the detector response was measured such that the normalized yield for same condition over a three month period indicated little change ($< 1\%$). These measurement were then used to show that for short time (20 minutes periods between target spin flip), the detector drift was estimated to be less than 1% times the ratio of the time period between target spin flip and three months. For the present experiment we use the same estimate except for the period between target polarization states used is $\sim$12 hours leading to an overall drift $d\varepsilon \sim 0.01\%$. A similar approach can be used to establish an estimate for dQ using studies from the data from the (g2p/GEp) experiment resulting in $d\varepsilon \sim 0.01\%$.

To express A_{zz} in terms of the estimated experimental drifts in efficiency and current measurement we can write,

$$A_{zz} = \frac{2}{fP_{zz}}\left(\frac{N_1}{N} - 1\right) \pm \frac{2}{fP_{zz}}d\xi. \tag{13}$$

This leads to a contribution to A_{zz} on the order of 1×10^{-3},

$$dA_{zz}^{drift} = \pm\frac{2}{fP_{zz}}d\xi = \pm 3.7 \times 10^{-3}. \tag{14}$$

Though a very important contribution to the error this value allows a clean measurement of $A_{zz} = 0$ at $x = 0.45$ without overlap with the Hermes error bar. For this estimate we assume only two

	E_0 (GeV)	Q^2 (GeV^2)	W (GeV)	E' (GeV)	$\theta_{e'}$ (deg.)	Rates (kHz)	PAC Time (hours)
SHMS	8.8	1.5	0.46	8.36	8.2	0.55	600
SHMS	6.6	0.7	0.60	6.50	8.2	4.08	90
SHMS	2.2	0.3	0.87	2.11	14.4	3.73	30
HMS	2.2	0.3	0.86	2.11	14.9	4.65	30

Table 2: Summary of the kinematics and physics rates using the Hall C spectrometers.

polarization state changes in a day. If it is possible to increase this rate then the systematic effect in A_{zz} will decrease accordingly.

Naturally detector efficiency can drift for a variety of reasons, for example including fluctuations in gas quality, HV drift or drifts in the spectrometers magnetic field. All of these types of variation as can be realized both during the experiment though monitoring as well as systematic studies of the data collected.

It can be difficult to know changes in luminosity, however the identical condition of the two polarization states minimizes the relative changes in time. There are also checks on the consistency of the cross section data that can be use ensuring the quality of each run used in the asymmetry analysis. Each of these systematic effects can mitigate the systematic uncertainty to ~ 0.001, which is required for the b_1 measurement. In the kinematic region proposed here, A_{zz} is expected to be much larger, on the order of 0.1 to 1.0. While typical false asymmetries in Hall C of 0.01 are acceptable for this proposed measurement, it can also allow for a test of the methods used to reduce them further.

1.2 Kinematics

We will measure the tensor asymmetry A_{zz} for $0.80 < x < 1.75$, 1.0 (GeV/c)^2 $< Q^2 <$ 1.9 (GeV/c)^2, and $0.59 < W < 1.09$ GeV. Fig. 2 shows the planned kinematic coverage utilizing the Hall C HMS and SHMS spectrometers at forward angle.

The polarized ND_3 target is discussed in section **??**. The magnetic field of the target will be held constant along the beamline at all times, while the target state is alternated between a polarized and unpolarized state. The tensor polarization and packing fraction used in the rates estimate are 30% and 0.65 , respectively. The dilution fraction changes with x in the range of this measurement as shown in Fig. 3. With an incident electron beam current of 115 nA, the expected deuteron luminosity is $?.?? \times 10^{35}$ cm^{-2}s^{-1}.

The momentum bite and the acceptance were assumed to be $\Delta P = \pm 8\%$ and $\Delta\Omega = 5.6$ msr for the HMS, and $\Delta P = ^{+20\%}_{-8\%}$ and $\Delta\Omega = 4.4$ msr for the SHMS. For the choice of the kinematics, special attention was taken onto the angular and momentum limits of the spectrometers: for the HMS, $10.5^\circ \leq \theta \leq 85^\circ$ and $1 \leq P_0 \leq 7.3$ GeV/c, and for the SHMS, $5.5^\circ \leq \theta \leq 40^\circ$ and $2 \leq P_0 \leq 11$ GeV/c. In addition, the opening angle between the spectrometers is physically constrained to be larger than 17.5°. The dilution factors and projected uncertainties in A_{zz} are

	$Q^2 = 1.5$ (GeV/c)^2			$Q^2 = 0.7$ (GeV/c)^2			$Q^2 = 0.3$ (GeV/c)^2		
x	f_{dil}	δA_{zz}^{stat} $\times 10^{-2}$	δA_{zz}^{sys} $\times 10^{-2}$	f_{dil}	δA_{zz}^{stat} $\times 10^{-2}$	δA_{zz}^{sys} $\times 10^{-2}$	f_{dil}	δA_{zz}^{stat} $\times 10^{-2}$	δA_{zz}^{sys} $\times 10^{-2}$
0.80	0.205	0.52	0.53	0.175	0.63	0.53	0.298	0.41	0.53
0.90	0.274	0.39	1.20	0.375	0.27	1.20	0.462	0.25	1.20
1.00	0.507	0.21	0.05	0.518	0.19	0.05	0.521	0.24	0.01
1.10	0.333	0.42	1.75	0.409	0.31	1.42	0.431	0.35	1.16
1.20	0.174	1.13	3.51	0.264	0.66	2.85	0.301	0.65	2.32
1.30	0.120	2.32	5.26	0.174	1.26	4.27	0.193	1.18	3.48
1.40	0.127	3.61	7.01	0.156	2.18	5.69	0.144	1.91	4.64
1.50	0.096	5.81	8.77	0.170	2.93	7.12	0.100	3.19	5.81
1.60	0.096	7.93	10.0	0.110	4.86	8.54	0.086	4.09	6.97
1.70	0.095	10.7	10.0	0.096	6.97	9.96	0.063	6.30	8.31
1.80	0.096	13.7	10.0	0.096	9.13	10.0	0.056	7.72	9.29

Table 3: Summary of the expected statistical uncertainty after combining overlapping x-bins. Values represent the statistics weighted average of all events that satisfy our kinematic cuts.

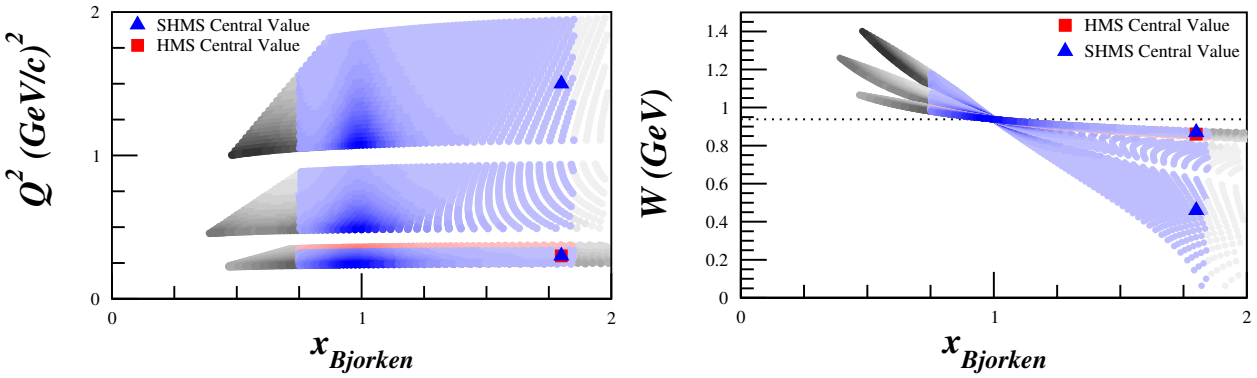

Figure 2: Kinematic coverage. The grey settings are not included in our rates estimates since they fall outside of $0.80 < x < 1.75$. The highlighted represent the central value of the spectrometer setting, which are not the statistics weighted average of the distribution. The shading represents areas with relative statistics for each setting.

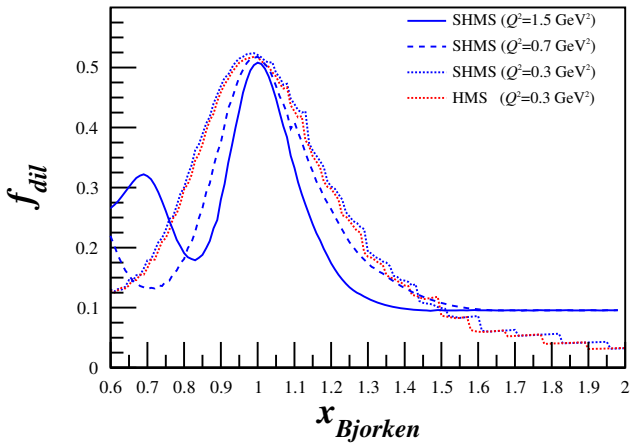

Figure 3: Projected dilution fraction covering the entire x range to be measured using a combination of the Bosted [3] and Sargsian [**?**] code for the SHMS and HMS.

summarized in Table 3 and displayed in Fig. 4.

A total of 30 days of beam time is requested for production data, with an additional 5 days of expected overhead.

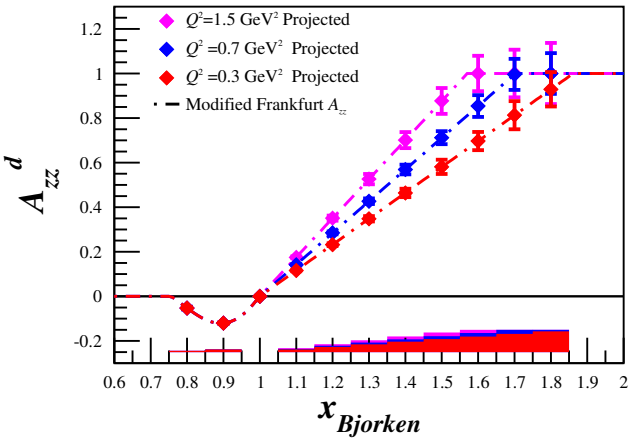

Figure 4: Projected statistical errors for the tensor asymmetry A_{zz} with 30 days of beam time. The band represents the systematic uncertainty. Also shown is the Frankfurt and Strikman model [1] that has been modified to estimate the plateau changing with Q^2.

References

[1] L. Frankfurt and M. Strikman, Phys.Rept. **160**, 235 (1988).

[2] D. Keller, "Uncertainty in DNP Target Data for E08-007", JLab-TN-12-051.

[3] P. Bosted and V. Mamyan, (2012).